Nanoscale

Accepted Manuscript

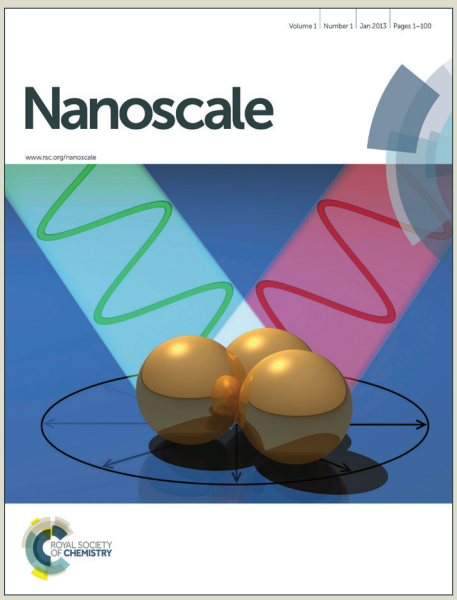

ROYAL SOCIETY OF CHEMISTRY

www.rsc.org/nanoscale

Nonvolatile optically-erased colloidal memristors

Christopher F. Huebner[†,‡], Volodymyr Tsyalkovsky[†], Yuriy Bandera[†], Mary K. Burdette[†], Jamie A. Shetzline[§], Charles Tonkin[‡], Stephen E. Creager[§], and Stephen H. Foulger[†,♮,*]

Center for Optical Materials Science and Engineering Technologies
[†]Department of Materials Science and Engineering
[‡]Sonoco Institute of Packaging Design and Graphics
[§]Department of Chemistry
[♮]Department of Bioengineering
Clemson University, Clemson, SC 29634-0971, USA

[*]To whom correspondence should be addressed; e-mail: foulger@clemson.edu.

September 5, 2014

KEYWORDS: flexible electronics, printing, nonconjugated methacrylate terpolymer, carbazole, 1,3,4-oxadiazole

Abstract

A nonconjugated methacrylate terpolymer containing carbazole moieties (electron donors), 1,3,4- oxadiazole moieties (electron acceptors), and Coumarin-6 in the pendant groups was synthesized via free radical copolymerization of methacrylate monomers containing the respective functional groups. The terpolymer was formed into 57 nm particles through a mini-emulsion route. For a thin 100 nm film of the fused particles sandwiched between an indium-tin oxide (ITO) electrode and an Al electrode, the structure behaved as a nonvolatile flash (rewritable) memory with accessible electronic states that could be written, read, and optically erased. The device exhibited a turn-on voltage of ca. -4.5 VDC and a 10^6 current ratio. A device in the ON high conductance state could be reverted to the OFF state with a short exposure to a 360 nm light source. The development of semiconducting colloidal inks that can be converted into electroactive devices through a continuous processing method is a critical step in the widespread adoption of these 2D manufacturing technologies for printed electronics.

1 Introduction

Printing is a process converging in on traditional manufacturing techniques with the advent of functional, processable nanoscale materials. A significant portion of consumer goods with some form of decorative printing is created through a roll-to-roll process since these 2D manufacturing technologies are well established as a commercial industry and can produce goods at a very high volume & low cost. Functional printing, which includes printed electronics, is a disruptive technology that is growing rapidly in currently five recognized disciplines: lighting; organic photovoltaics; flexible displays; electronics and components (including RFID, memories, batteries and other components); and integrated smart systems (including smart objects, sensors and smart textiles)[1-3]. Printed electronics predominately relies on electrically active organic or polymeric colloidal inks that can be employed in a variety of designations, such as conductors, semiconductors, luminescent, electrochromic, or electrophoretic roles.

A polymeric layer sandwiched between two aligned electrodes that can be modulated by an electrical stimulation into two stable resistance states constitutes a simple memory design. This new device alters its conductivity based on its electronic history and is referred to as a memory resistor or "memristor"[4]. In this implementation, instead of encoding "0" and "1" as the amount of charge stored in a traditional silicon-based cell, the low and high conductivity condition is interpreted as the OFF and ON states. This voltage path dependence can be exploited in a collection of circuit elements to achieve adaptive network systems[5]. One of the very appealing aspects of this device is that both information retention and processing could be combined in a single printed device, a potentially massive advantage for the electronic printing community in achieving a reduced decoder size.

There are a number of non-conjugated polymers that have been developed which are based on acrylates that have pendant carbazoles and exhibit

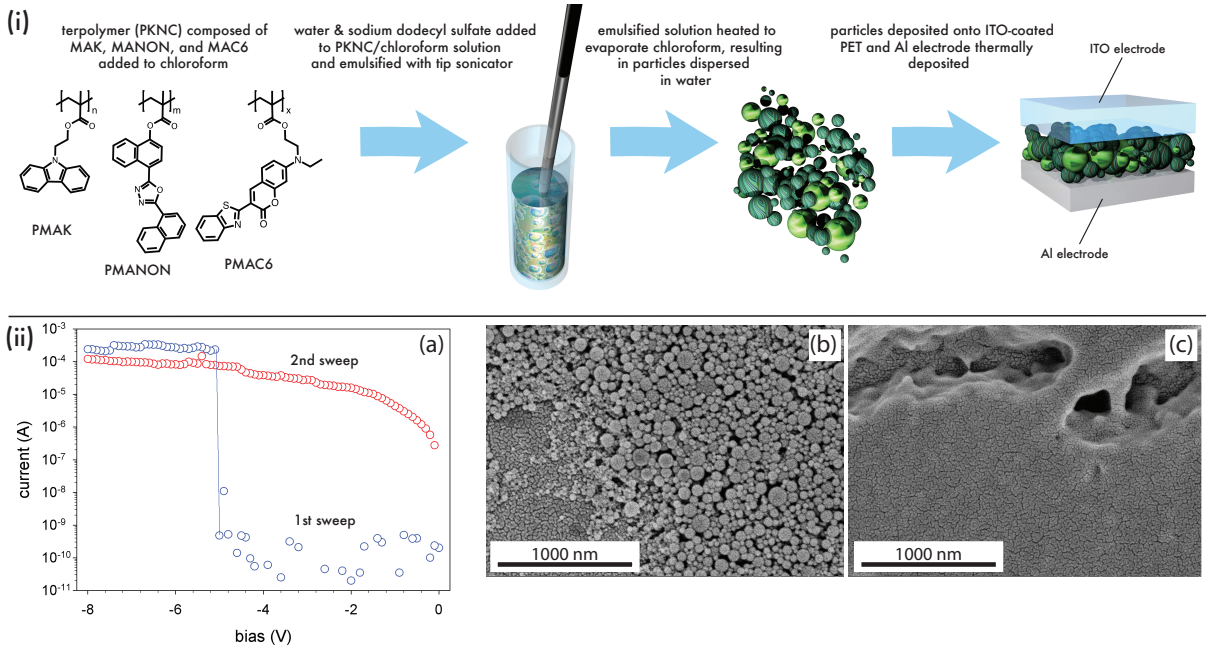

Figure 1: **(i)** Procedure for converting terpolymer (PKNC) of 2-(9*H*-carbazol-9-yl)ethyl methacrylate (MAK); 4-[5-(1-naphthyl)-1,3,4-oxadiazol-2-yl]-1-naphthyl methacrylate (MANON); and methyl methacrylate derivatized with Coumarin-6 (MAC6) into colloids and fabricating memory device. The copolymer of MAK and MANON is designated as PKN. **(ii) (a)** Current-voltage characteristics of PKNC colloidal device. Device structure was ITO(150 nm)/colloid(100 nm)/Al(200 nm) and was annealed at 140 °C for 24 hours prior to testing. SEM micrograph of colloids **(b)** as-deposited and **(c)** annealed; image taken at edge of sample for depth perspective.

volatile and non-volatile bistablity conductance[6, 7]. One specific polymer employed as memory is 2-(9*H*-carbazol-9-yl)ethyl methacrylate (MAK) where conformational change of the pendant carbazoyl groups is the proposed mechanism in the conductance bistability[6]. Field induced conformational changes in polymers has been indicated to be a prime mechanism for resistive switching in polymers with pendant electronic conjugation. This mechanism for resistive switching relies on the molecular mobility of the pendant groups to allow "islands" of electronic delocalization to spatially readjust to allow charge tunneling or transport between islands under an applied field. Unlike poly(9-vinylcarbazole) (PVK), which exhibits only a high conductance condition (ON state) due to the rigidity of the carbazole rings adjacent to the polymer backbone, the carbazole rings in PMAK have a longer linkage and are spaced away from the backbone which affords them a degree of freedom. For PMAK, its been proposed[8] that when an applied voltage (and corresponding electric field) exceeds a threshold value, a fraction of the carbazole groups undergo a conformational alignment, resulting in enhanced charge transport through spatially adjacent carbazole groups either on the same or neighboring polymer chains. The aligned rings offer a percolation path for charge transport through the sample resulting in a high conductivity state (ON state). With the cessation of the electric field, the charged rings, which are stabilized by the adjacent electron-withdrawing ester groups, do not return to their unaligned state. In PMAK memory, the devices were nonvolatile and could not be returned to the OFF state by the application of a reverse erasing bias of magnitude similar to or higher than the switching voltage and therefore behaves as a write-once read-many-times (WORM) electronic memory. The structurally similar polymer composed of 9-(4-vinylphenyl)carbazole (VPK) exhibited a single high conductance state, similar to PVK. Copolymerizing VPK with less than 20 % (mole) of an electron-accepting 1,3,4-oxadiazole containing monomer resulted in volatile memory[7]. The lower energy level of the HOMO level of the oxadiazolyl-containing monomers relative to the carbazolyl-containing monomer ($\Delta E \sim 0.4$ - 0.53 eV) was speculated to act as trap sites for charge carriers. These hole-blocking moieties were responsible for the devices exhibiting conductance switching[7]. In the current effort, a terpolymer containing methyl methacrylate monomers modified with either a carbazole, oxadiazol, or UV/Vis fluorescent moiety was employed as the active material in a memory device. The resulting system was a nonvolatile elec-

tronic memory that could be optically erased. In addition, the terpolymer could be engineered into aqueously dispersed colloids that could be employed as a roll–to–roll printable memristive ink.

2 Results and Discussion

Figure 1(i) presents a schematic of the materials and methods employed in this effort. The terpolymer (PKNC) employed in the colloid-based memristor was composed of MAK, 4-[5-(1-naphthyl)-1,3,4-oxadiazol-2-yl]-1-naphthyl methacrylate (MANON), and a 3-(2-benzothiazolyl)-7-(diethylamino)coumarin (Coumarin-6) derivative of MA (MAC6). The resulting terpolymer exhibited a molar ratio of MAK/MANON/MAC6 of 69.3/29.7/1 and glass transition of 156 °C. The resulting polymer was formed into colloids utilizing the versatile "mini-emulsion" process[9]. In this process, the water-insoluble PKNC polymer was dissolved in chloroform and then a solution of water & sodium dodecyl sulfate was added. Sonication and a subsequent evaporation of the chloroform results in the formation of polymeric particles dispersed in an aqueous environment. The scanning electron micrograph (cf. Figure 1(ii)b) presents a typical batch of the colloids after dialysis to clean the particles. Based on the micrograph in Figure 1(ii)b, the colloids range in diameter from 20 nm up to 130 nm. The mean particle diameter was 57 nm, but unlike a more traditional emulsion polymerization[10, 11], the polydispersity was significant relative to the mean diameter and resulted in a standard deviation of 26 nm. The memory device was formed by depositing the colloids via spin-coating or a screen bar into a ca. 100 nm layer sandwiched between a 150 nm thick indium- tin-oxide (ITO) anode and a thermally-evaporated 200 nm thick aluminum cathode with active area of 3 x 4 mm^2.

The typical electrical conductivity switching and memory effects of a colloid-based PKNC device is illustrated by the current versus voltage, or I-V characteristics, in Figure 1(ii)a. In the initial voltage sweep, the ITO was kept at 0 VDC while the potential on the Al electrode was swept from zero to -8 VDC. The corresponding current flow in the device hovered around 10^{-10} A, the lower resolution of the semiconductor analyzer, up to bias of ca. -4.8 VDC, at which point, the current dramatically increased to 10^{-4} A, for a 6 orders of magnitude total change. Continuing to increase the bias on the device beyond -5 VDC up to -8 VDC resulted in a relative static current trace at $2x10^{-4}$ A.

A second voltage sweep between 0 VDC and -8 VDC resulted in a current flow that was significantly different relative to the initial cycle. The second current trace was relatively flat, exhibiting a value of $4x10^{-6}$ A at -1 VDC and increasing up to $1.2x10^{-4}$ A at -8 VDC. In this second cycle, at a voltage of -2 VDC, the current flow is approximately six orders of magnitude greater than the previous cycle. With any subsequent cycle between 0 VDC and -8 VDC, the current retraced the second cycle profile. Clearly, the exposure of the device to a bias greater than ca. -4.8 VDC on the first sweep has altered the voltage-current characteristics of the sample. Through the analysis of a number of samples, it was determined that the devices experienced a "turn on" voltage (V_{ON}) between -4.5 VDC and -5 VDC. The device is considered in its OFF state when it has never been exposed to a potential greater than V_{ON}, and it is in its ON state once it has been swept through a voltage of at least V_{ON}. The currents are in the mA and nA range when the devices are in their ON and OFF states, respectively.

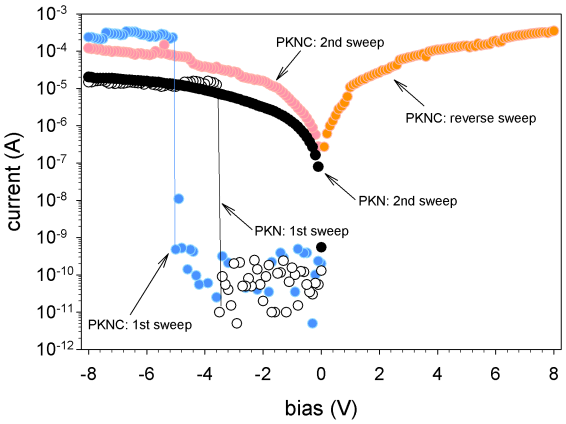

Figure 2: Current-voltage characteristics of PKNC and PKN colloidal device. Device structure was ITO(150 nm)/colloid(100 nm)/Al(200 nm) and was annealed at 140 °C for 24 hours prior to testing. ITO was kept at 0 VDC while the potential on the Al electrode was swept from zero to -8 VDC.

The ±0.5 VDC variability in V_{ON} seen in the devices was attributed to both material intrinsic properties as well as the sample preparation techniques. The colloids were deposited on the ITO-coated PET substrates through both spin coating and a screen bar (to mimic roll-to-roll printing) to achieve a ca. 100 nm colloid layer. This thickness was achieved by only a few stacked particles, as indicated in Figure 1(ii)b. This was then annealed at 140 °C, slightly below the glass transition temperature, for 24 hours to fuse the edges of the particles together (cf. Figure 1(ii)c) prior to metalization to prevent pin-hole formation. The resulting devices exhibited an active layer thickness that ranged from ca. 80 nm to 120 nm. This variation in thickness, and corresponding

electric field, was considered a contributing factor to the observed range in turn-on voltages.

Previous efforts with an oxadiazole & 9-(4-vinylphenyl) carbazole (VPK) copolymer resulted in material with a bistable conductance state, but the ON state would revert within minutes to an OFF state without a refreshing voltage pulse[7]. Since the VPK homopolymer exhibited only a high conductance state, it was speculated that the inclusion of the oxadiazole moieties into the polymer created shallow traps due to the HOMO energy mismatch between the carbazoles and oxadiazoles, contributing to an unstable ON state. The current PKNC system did not exhibit a return to the OFF state even after several days after being exposed to a potential greater than V_{ON}. In addition, as Figure 2 presents, once the rings have aligned at V_{ON} to create a charge carrier pathway, charge transport under both biases is supported and the elevated conductance is not switched off with a reverse bias sweep or the application of a higher voltage of the same bias. In order to elucidate the influence of the MAC6 in the terpolymer, the copolymer of MAK and MANON (PKN) was studied, where the MAK and MANON were in a 70/30 molar ratio, respectively. The system exhibited similar electrical properties to the terpolymer (cf. Figure 2) but exhibited only a 5-order of magnitude change in current at V_{ON}, relative to the 6-order of magnitude change seen with the PKNC terpolymer. In addition, V_{ON} for the copolymer (PKN) was approximately one volt less than the terpolymer (PKNC) at ca. 3.5 VDC. This enhancement in current ratio has been previously seen in other dye-modified polymeric memristors[12]. Surprisingly, the PKN memory was nonvolatile and the second trace presented in Figure 2 was conducted 6 days after the memory was turned on.

In an amorphous semiconducting polymer, the concept of extended state energy bands is replaced with localized states described by the lowest unoccupied molecular orbital (LUMO) and the highest occupied molecular orbital (HOMO). Traps are defined as preferred energy states that are situated in the energy gap of the semiconductor by the inclusion of, for example, dopants. As indicated earlier, previous efforts have employed the use of oxadiazoyl moieties into a VPK-rich polymer to create shallow traps due to the HOMO energy mismatch between the carbazoles and oxadiazoles to fabricate volatile memory from the single conductance state PVPK homopolymer[7]. The electrochemical characteristics of homopolymers derived from the monomers (i.e. PMAK, PMANON, and PMAC6) were investigated through cyclovoltammetry (CV) to estimate their corresponding HOMO energy levels[13]. Figure 3

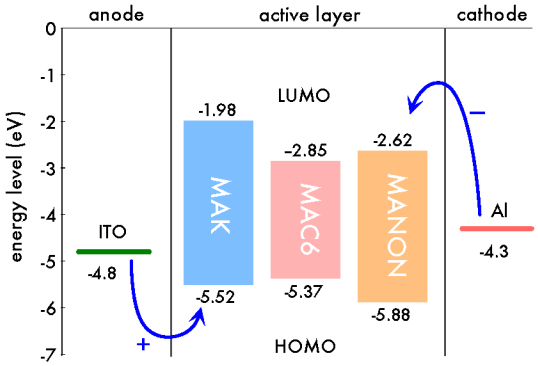

Figure 3: Electronic characteristics of PMAK, PMAC6, and PMANON polymers measured by UV-vis spectroscopy and cyclovoltammetry; all energies expressed in eV and are relative to the vacuum level. LUMO values based on the difference of the measured oxidation potential (HOMO) and energy at experimentally observed electronic absorption band edge.

presents the experimentally-derived energy levels of the homopolymers relative to the device electrodes. Since no reversible reduction process is observed for these polymers, the LUMO energy levels were estimated from the HOMO values and the optical absorption band edge; Figure 4 presents the optical absorption and photoluminescence of the monomers employed in the PKNC terpolymer. As expected, polymerization of the monomers did not result in significantly different absorption spectra (data not presented)[14]. The energy difference between the HOMO and LUMO of the terpolymer and the work function of the metal electrodes will result in Schottky barriers being formed at both the Al/PKNC and PKNC/ITO interfaces[15]. The negative voltage sweeps with ITO as the anode, holes are injected from the ITO electrode and electrons are injected from the Al electrode. The MAK accounts for 70 % of the repeat residues in the terpolymer and should account for the majority of the percolative pathways. This is coupled to the fact the energy barrier at the ITO/MAK (HOMO level) contact is relatively low at 0.72 eV, when compared to the 1.68 eV barrier at the Al/MANON (LUMO level) contact. Due to the low energy barrier of the ITO/MAK interface and preponderance of MAK residues in the terpolymer, the hole injection from ITO into the HOMO level of the random terpolymer should be the dominant process and the PKNC can be described as a hole-transporting material. The interactions between carbazole and oxadiazole are relatively weak by the lack of new bands in the absorption spectra[14] thus we would expect they keep their HOMO/LUMO position independent of the surrounding matrix. If the major-

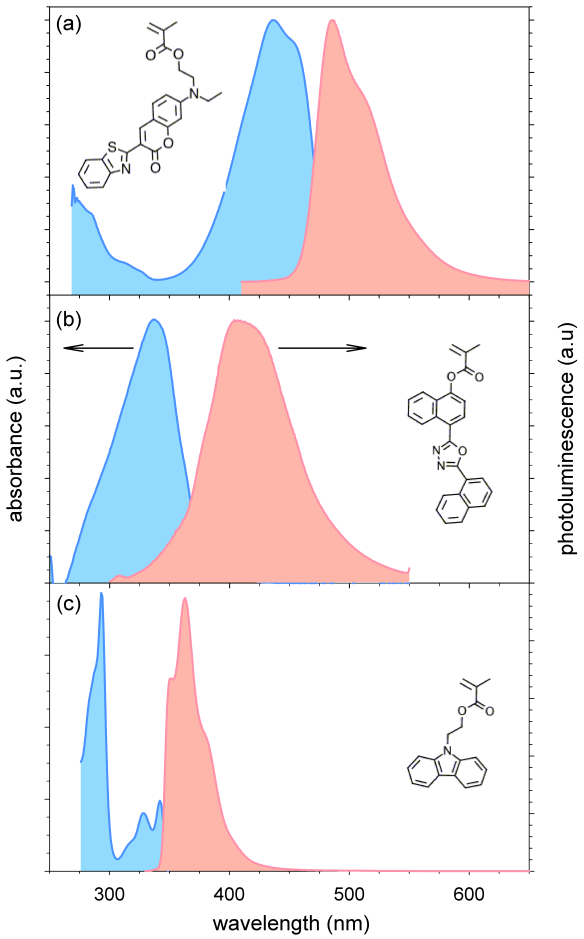

Figure 4: Absorbance and photoluminescence spectra of (**a.**) MAC6, (**b.**) MAON, and (**c.**) MAK in THF. Solutions at a monomer concentration of 1.0 mg/ml; excitation wavelength of 315 nm.

ity matrix, in the current case the MAK, is "doped" with a second molecule that has a HOMO or LUMO that is positioned in the gap of MAK it will form charge trap sites. The current PKNC active layers are predominately hole transports and a trap in the case would be an energy state greater than MAK's HOMO energy. The MAC6 residues fulfill this trap criteria having a 0.15 eV higher HOMO energy relative to the MAK. In contrast, the MANON residues have HOMO energies that are lower than MMAK by 0.36 eV and would act more like a hole scattering centers than as traps[16]. Previous studies on the structurally similar PVK indicated that the majority of traps in this homopolymer are at an energy depth of about 200 meV and are related to excimers, but with the addition of a small molecule oxadiazole, the majority of traps become shallower and are attributed to exciplexes formed between the carbazole and oxadiazole moieties[17].

Initially when the PKNC or PKN device is biased at a low negative voltage, holes are injected at the Schottky barrier which is located near the anode and oxidizes the carbazole groups near the interface, forming positively charged species[8, 6]. Spatially adjacent neutral carbazole groups undergo donor-acceptor interactions with the positively charged carbazole groups resulting in rotation of the rings into a partial or full face overlap. This leads to an accumulation of space charge and a redistribution of the electric field[15]. The process is propagated throughout the film and, near the turn-on voltage, a significant fraction of the carbazole groups has undergone such a conformational change. The ordered carbazole groups, either on the same or neighboring polymer chains, results in an enhanced charge transport via intra- or inter-chain hopping producing the high conductivity state (ON state). When the device is de-energized, the partial positive charge localized on the carbazoles is stabilized by the electronegative oxygen in the ester linkages and oxadiazoles resulting in nonvolatile memory (cf. Figure 2)[18]. Once the rings have aligned at V_{ON} to create a charge carrier pathway, the elevated conductance is not switched off with a reverse bias sweep or with the application of a higher voltage of the same bias and the ON device exhibits Ohmic behavior with a resistance of 10^5 Ω. The localized positive charge on the nitrogen of the carbazole elevates the HOMO and decreases the LUMO energy levels of the carbazole moieties relative to the electrodes. This results in an almost symmetrical I-V curves under both biases (cf. Figure 2) in spite of the difference in energy barriers for hole injection under different voltage biases, which is 0.8 eV for hole injection from Al into the HOMO under positive bias and 0.7 eV for hole injection from ITO into the HOMO under negative bias.

In the PKNC terpolymer, the MAC6 is a strongly fluorescent moiety with an absorption peak at ca. 425 nm and an emission peak at ca. 500 nm. Assuming that the PKNC device in the high conductance state is conformationally stabilized by electrostatic interactions of the three polymer repeat units, the active layer could be potentially "flushed" of trapped carriers by an excitation probe at a wavelength of 450 nm or by energy transfer from the optically excited oxadiazole moieties, resulting in a redistribution of the electric field and return to the OFF state[19, 20]. Based on their absorption/luminance spectra (cf. Figure 4), the MAON and MAC6 monomers are a good donor/acceptor pair. A donor/acceptor pair that exhibits overlap in the donor's fluorescence (MAON)

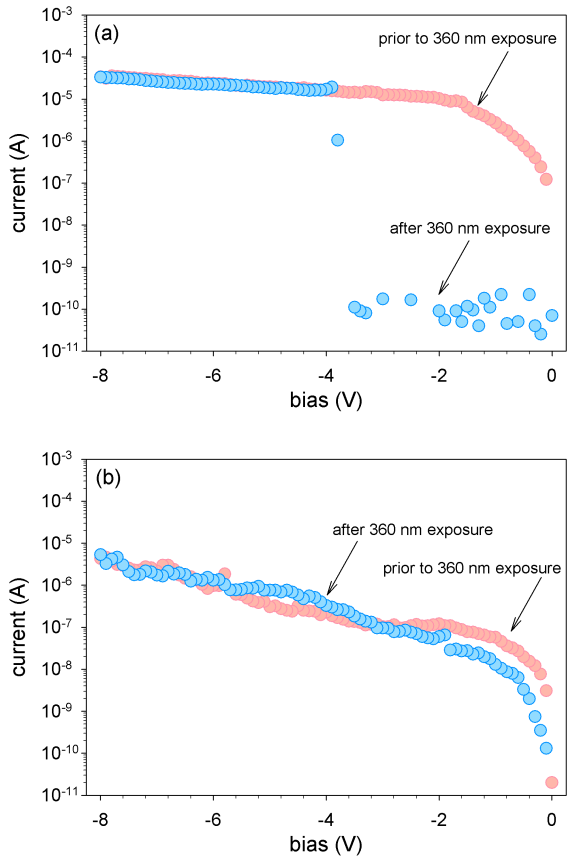

Figure 5: Current-voltage characteristics of turned *ON* (**a.**) PKNC and (**b.**) PKN colloidal device before (red) and after (blue) 2 min exposure to 360 nm light source.

and the acceptor's absorption (MAC6) spectra and which are spaced within the Förster radius (Förster resonance energy transfer (FRET)) can be used to achieve energy transfer. Since the molar ratio of the MAON is significantly higher than the MAC6 in the terpolymer, pumping into this monomer and then using FRET to the chromophore is a route to achieve a high energy flux to the MAC6. Using a device which had undergone voltage switching and was in the ON state, a 360 nm light was used to excite the oxadiazoles for 2 minutes which resulted in FRET to the MMC6 and a strong green fluorescence. Figure 6 presents the photoluminence (PL) of both the PKNC and PKN colloidal device in the ON state; the lower energy shoulders in the PL spectra relative to the MANON and MAC6 repeat units (cf. Figure 4) are indicative of exciplex formation. The resulting device then underwent a second voltage sweep in the dark. Figure 5a presents the *I-V* curve of the terpolymer PKNC device. During the initial negative voltage sweep, prior to the 360 nm exposure, the device is in the ON state. The second voltage sweep, after the illumination of the device with 360 nm light, clearly indicates that the device is in the OFF state and exhibits the typical transition to the ON state at ca. -4 VDC. The nonvolatile memory in the PKNC device has been optically erased. Performing the same procedure with a PKN device (cf. Figure 5b) did not result in a loss of the high conductance state. Since both the PKNC and PKN devices only differ by a 1 mole % of the MAC6 repeat unit, photoexcited excitons generated on this moiety may be recombining with the positively charged carbazoles resulting in a redistribution of the local electric field[21]. This redistribution initiates a randomization of the carbazole ring orientations. The reorientations results in a loss of percolation and return to the OFF state.

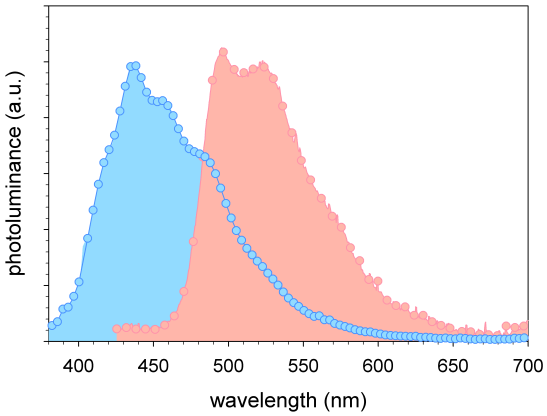

Figure 6: Photoluminescence of PKNC (red) and PKN (blue) colloidal device in the ON state with excitation at 360 nm. Device structure was ITO(150 nm)/colloid(100 nm)/Al(200 nm).

3 Conclusion.

In the bulk PKN or PKNC polymer, charge carriers are assumed to have a higher intra- & inter-chain mobility when the overlapping of related orbitals is large between two adjacent carbazole or oxadiazole rings[22, 23]. Achieving this overlap is directly related to the local electric field that the moieties experience that force them to adopt an overlapping conformation, ultimately dictating the turn-on voltage. In an amorphous polymer, the local environments of the pendant moieties are vastly different and the activation energies to rotate the rings would be a spectrum of values. It is unreasonable that a direct "immediate" rotation of the rings occurs. Its more likely that the degree of electronic overlap exhibits a percolation threshold at which sufficient rings are in electronic contact that the conductance throughout the bulk material is guaranteed and the current levels

jump to the ON state. The observed difference in the memristor performance with the random addition of a minute quantity of the MAC6 repeat unit to the PKN copolymer (i.e. PKNC) is attributed to the decrease in a finite number of the carbazole's (and oxadiazole's) rotational activation energies. This is coupled with the propensity of the MAC6 moieties to stabilize the overlapping rings, via charge trapping. With a UV excitation, the photogenerated charges from the MAC6 allow for a redistribution of the electric field and a loss of percolative ring overlap, resulting in a return to the OFF state. These particles will build upon the growing library of semiconducting colloidal inks that can be converted into electroactive devices through a continuous processing method, such as roll-to-roll printing, aiding the widespread adoption of these 2D manufacturing technologies for printed electronics.

4 Experimental.

4.1 Reagents and solvents.

All the commercial reagents were used without further purification. All the solvents were dried according to standard methods. Deionized water was obtained from a Nanopure System and exhibited a resistivity of ca. 10^{18} ohm^{-1}cm^{-1}. Aluminum (Al) (99.9%) were purchased from Kurt J. Lesker Co. and used without further purification. Indium tin oxide (ITO) coated glass slides, 156.25 mm^2, were purchased from Delta Technologies, Inc.

4.2 Characterization.

^{1}H and ^{13}C NMR spectra were recorded on JEOL ECX 300 spectrometers (300MHz for proton and 76MHz for carbon). Chemical shifts for protons are reported in parts per million downfield from tetramethylsilane and are referenced to residual protium in the NMR solvent ($CDCl_3$: δ 7.26 ppm, DMSO-d6: δ 2.50 ppm). Chemical shifts for carbons are reported in parts per million downfield from tetramethylsilane and are referenced to the carbon resonances of the solvent ($CDCl_3$: δ 77.16, DMSO-d6: δ 39.52 ppm). Photoluminescence (PL) spectra were collected using a Jobin-Yvon Fluorolog 3-222 Tau spectrometer.

The electrochemical characteristics of the materials were investigated through cyclovoltammetry (CV) to estimate their corresponding HOMO energy levels. This was performed by using an ITO-coated glass slide as the working electrode which had a thin film of the polymer of interest deposited on it, an Ag/AgCl reference electrode, and a platinum wire as a counter electrode. CV measurements were conducted in a 0.1 M $LiClO_4$ acetonitrile solution at room temperature with a scan rate of 50 mV/s; the electrochemical cell was calibrated against ferrocene and the half-wave potential was estimated to be 400 mV against an Ag/AgCl reference[24]. The LUMO energies were based on the difference of the measured oxidation potential (HOMO) and the energy at the experimentally observed electronic absorption band edge.

4.3 Materials

Monomer preparation.

See Figure 7 for synthetic scheme.

2-(9*H*-carbazol-9-yl)ethyl methacrylate (MAK) 2-(9*H*-carbazol-9-yl)ethanol**(6)** (15 g, 71 mmol) was dissolved in dichloromethane (50mL). Triethylamine (12.4 ml, 89 mmol) was added, and the reaction mixture was allowed to stir in an ice bath for 30 min. Methacryloyl chloride (8.7 ml, 89 mmol) was slowly added over a period of 10 minutes. Afterwards, the ice bath was removed and the mixture was allowed to stir at room temperature for 2 h. The reaction mixture was then washed with water and brine; the resulting organic phase was dried over anhydrous sodium sulfate. The organic layer was then filtered and dried under reduced pressure. The product was then reprecipitated in methanol 3-4 times and dried in a vacuum oven at 70 °C. Yield: 17.8 g (90%). Melting Point (by DSC): 86 °C. MS m/z = 279 (M+). ^{1}H NMR ($CDCl_3$, δ): 8.13 (d, 2H), 7.47 (m, 4H), 7.26 (m, 2H), 5.94 (s, 1H), 5.48 (s, 1H), 4.63 (t, 2H), 4.55 (t, 2H), 1.82, (s, 3H).

3-(ethylamino)phenol (1a)

Dry diethyl ether (400 mL) was placed in a 1 L round bottom flask; the flask was purged with nitrogen. $LiAlH_4$ (6.4 g, 168.4 mmol) was added slowly, by portions, to the reaction vessel. Me_3SiCl (18.3 g, 168.7 mmol) was added to the reaction mixture dropwise. The reaction mixture was stirred for 15 min. Afterwards, a suspension of *N*-3hydroxyphenyl)acetamide (15 g, 99.2 mmol) in THF (100 mL) was added by portions over a period of 3 hours. The reaction mixture was then refluxed for 18 hours. A solution of DI water (12 mL) and tetrahydrofuran (THF, 35 mL) was added to the reaction vessel dropwise to hydrolyze the mixture . The reaction mixture was separated via filtration, and the solid was washed with dichloromethane; this mixture was also separated via filtration. The two filtrates were combined and evaporated under reduced pressure. The residue was mixed with dichloromethane; the mixture was filtered to remove the crystalized starting material. The filtrate was collected and evaporated

under reduced pressure. Yield: 7.5 g (55%). ^{1}H NMR ($CDCl_3$, δ): 7.01 (t, 1H, *J* 8 Hz), 6.19 (m, 2H, *J* 2.2 Hz, 8 Hz), 6.10 (t, 1H, *J* 2.2 Hz), 3.10 (q, 2H), 1.23 (t, 3H).

3-[ethyl(2-hydroxyethyl)amino]phenol (1b)

1a (9 g, 65.6 mmol) was dissolved in acetonitrile (90 ml). 2-bromoethanol (13.1 g, 105 mmol), water (40 mL), and calcium carbonate (19.6 g, 196.8 mmol) were added to the reaction mixture. The reaction mixture was heated to reflux for 72 h. The reaction mixture was then allowed to cool to room temperature and was extracted with ethyl acetate and washed with water. The organic layer was collected, dried over anhydrous sodium sulfate (Na_2SO_4), and filtered. The organic solution was dried under reduced pressure. The residue was dissolved in ethyl acetate and purified by passing the residue through aluminum oxide and washing the aluminum oxide with methanol. Both the ethyl acetate and methanol solutions were collected and were dried under reduced pressure to yield a dark brown residue. The residue was extracted once again with $CHCl_3$, dried with (Na_2SO_4), and evaporated under reduced pressure to obtain a dark brown oil. Yield: 7.7 g (86%); ^{1}H NMR ($CHCl_3$, δ): 7.05 (t, 1H, *J* 8.3 Hz), 6.34 (d.d, 1H, *J* 2.1 Hz, 8.3 Hz), 6.26 (t, 1H, *J* 2.1 Hz), 6.19 (d.d, 1H, *J* 2.1 Hz, 8.3 Hz), 3.77 (t, 2H, *J* 5.9 Hz), 3.42 (t, 2H, *J* 5.9 Hz), 3.36 (q, 2H, *J* 6.9 Hz), 1.13 (t, 3H, *J* 6.9 Hz).

3-{[2-(acetyloxy)ethyl](ethyl)amino}phenyl acetate (1c)

1b (5 g, 27.6 mmol) was dissolved in 70 mL dry THF and covered with a septum. The reaction vessel was purged with nitrogen, and the reaction was carried out under a nitrogen atmosphere. Triethylamine (6.14 g, 60.7 mmol) was injected into the reaction vessel. The reaction vessel was placed in an ice bath and acetyl chloride (4.8 g, 60.7 mmol) was injected drop wise into the reaction vessel. The reaction mixture was allowed to warm up gradually to room temperature as the ice melted and was stirred for 14 h. The reaction mixture was subsequently quenched with water and was extracted with ethyl acetate and washed with water (2 x 100 mL). The organic layer was collected, dried over Na_2SO_4, and filtered. The organic layer was dried under reduced pressure. Yield: 6.3 g (86%); ^{1}H NMR ($CHCl_3$,δ): 7.19 (t, 1H, *J* 8.3 Hz), 6.56 (d.d, 1H, *J* 2.1 Hz, 8.3 Hz), 6.39 (m, 2H, *J* 2.1 Hz), 4.21 (t, 2H, *J* 6.2 Hz), 3.53 (t, 2H, *J* 6.2 Hz), 3.38 (q, 2H, *J* 6.9 Hz), 2.29 (s, 3H), 2.05 (s, 3H), 1.17 (t, 3H, *J* 6.9 Hz).

4-[ethyl(2-hydroxyethyl)amino]-2-hydroxybenzaldehyde (1d)

Phosphoryl chloride (2.9 mL, 30.9 mmol) was introduced drop wise to 10 mL dry N,N-dimethylformamide (DMF) at 30°C. The reaction mixture was stirred for 40 minutes, and then **1c** (6.3 g, 23.7 mol) was dissolved in 10 mL dry DMF and added drop wise to the reaction mixture. The mixture was stirred for 14 hours, then phosphoryl chloride (2 mL) dissolved in DMF (5 mL) was added to the reaction mixture. The reaction mixture was stirred at 30° for an additional 12 h. The reaction mixture was subsequently quenched with water (150 mL) and neutralized by adding an aqueous ammonia solution. pH was monitored via pH paper. After neutralization, the solution was extracted with ethyl acetate (70 mL), washed with water (1 x 100 mL), dried over Na_2SO_4, and filtered. The filtrate was dried under reduced pressure. The residue was dissolved in acetic acid (10 mL), hydrochloric acid (37%, 20 mL), and water (20 mL) and was heated at 80°C for 2 h. The reaction mixture was left at room temperature for 12 h then was quenched with water. The reaction mixture was neutralized by the addition of an aqueous ammonia solution. The reaction mixture was extracted with ethyl acetate, was washed with water (2 x 100 mL), and was dried over Na_2SO_4. The organic layer was dried under reduced pressure, and a dark brown oil was obtained. Yield: 2 g (40%); ^{1}H NMR ($CDCl_3$, δ): 9.51 (s, 1H), 7.29 (d, 1H, *J* 8.9 Hz), 6.32 (d.d, 1H, *J* 2.1 Hz, 8.9 Hz), 6.13 (d, 1H, *J* 2.1 Hz), 3.86 (t, 2H, *J* 5.9 Hz), 3.55 (t, 2H, *J* 5.9 Hz), 3.50 (q, 2H, *J* 6.9 Hz), 1.22 (t, 3H, *J* 6.9 Hz).

Ethyl 1,3-benzothiazol-2-ylacetate (2a)

2-aminobenzenethiol (3 g, 23.96 mmol) was mixed with ethyl cyanoacetate (2.71 g, 23.96 mmol), and the mixture was heated for 2 h at 120°C. Yield: 5.3 g (100%); ^{1}H NMR ($CDCl_3$, δ): 8.01 (d, 1H, *J* 8.6 Hz), 7.87 (d.d, 1H, *J* 1.4 Hz, 8.6 Hz), 7.36-7.50 (m, 2H, *J* 1.4 Hz, 8.6 Hz), 4.25 (q, 2H, *J* 7.2 Hz), 4.17 (s, 2H), 1.30 (t, 3H, *J* 7.2 Hz).

3-(1,3-benzothiazol-2-yl)-7-[ethyl(2-hydroxyethyl)amino]-2*H*-chromen-2-one (1e)

2a

(2.12 g, 9.56 mmol) and **1d** (2 g, 9.56 mmol) were dissolved in 20 mL of methanol. Piperidine (0.1 g) were added to the reaction mixture, and the reaction mixture was heated to reflux for 12 h. The reaction flask was allowed to cool to room temperature. Water (2 mL) was added to the solution and left for 48 h at room temperature. An orange solid precipitated, was filtered and washed with an 8:2 methanol:water solution (100 mL). Yield:

2.3 g (66%); ^{1}H NMR ($CDCl_3$, δ): 8.90 (s, 1H), 8.03 (d, 1H, *J* 8.3 Hz), 7.95 (d, 1H, *J* 8.3 Hz), 7.46-7.53 (m, 2H, *J* 1.4 Hz, 8.3 Hz, 8.9 Hz), 7.37 (m, 1H, *J* 1.4 Hz, 8.3 Hz), 6.74 (d.d, 1H, *J* 2.4 Hz, 8.9 Hz), 6.62 (d, 1H, *J* 2.4 Hz), 3.90 (t, 2H, *J* 2.4 Hz), 3.61 (t, 2H, *J* 5.2 Hz), 3.53 (q, 2H, *J* 6.9 Hz), 1.25 (t, 3H, *J* 6.9 Hz).

2-{[3-(1,3-benzothiazol-2-yl)-2-oxo-2*H*-chromen-7-yl](ethyl)amino}ethyl methacrylate (MAC6) [25]

Dry dichloromethane (50 mL) and triethylamine (0.22 g, 2.18 mmol) were added to 3-(1,3-benzothiazol-2-yl)-7-[ethyl(2-hydroxyethyl)amino]-2*H*-chromen-2-one (**1e**) (0.400 g, 1.09 mmol), creating a suspension. Methacryloyl chloride (0.23g, 2.18 mmol) was added to the reaction suspension. The suspension was stirred for 20 min at room temperature to allow all solids to dissolve. The reaction mixture was stirred an additional 24 h at room temperature. The mixture was extracted with dichloromethane, washed with water (2 x 100 mL), dried over Na_2SO_4, and vacuum filtered. The organic layer was dried under reduced pressure. The residue was dissolved in a 1:5 dichloromethane:hexanes solution. A red oil precipitated from the solution. The solution was decanted away from the red oil, and, upon decantation, yellow-orange crystals precipitated, which was the correct product. The product was dried between 40°C and 50°C under reduced pressure. Yield: 0.220 g (46%); ^{1}H NMR ($CDCl_3$, δ): 8.92 (s, 1H), 8.03 (d, 1H, *J* 7.9 Hz), 7.94 (d, 1H, *J* 7.9 Hz), 7.50 (m, 2H, *J* 8.3, 8.9 Hz), 7.37 (m, 1H, *J* 8.3 Hz), 6.77 (d.d, 1H, *J* 2.4, 8.9), 6.65 (d, 1H, *J* 2.4 Hz), 6.10 (s, 1H), 5.60 (t, 1H), 4.37 (t, 2H, *J* 6.2 Hz), 3.72 (t, 2H, *J* 6.2 Hz), 3.54 (q, 2H, *J* 6.9 Hz), 1.26 (t, 3H, *J* 6.9 Hz). ^{1}3C NMR ($CDCl_3$, δ): 167.37, 161.67, 161.03, 156.96, 152.69, 152.30, 142.06, 136.48, 135.90, 130.93, 126.54, 126.28, 124.72, 122.36, 121.77, 113.54, 110.32, 109.39, 97.77, 61.58, 48.99, 45.99, 18.47, 12.21.

5-(4-methoxynaphthalen-1-yl)-2H-tetrazole (3a) 4-methoxy-1-naphthonitrile, sodium azide (14.65 g, 225 mmol), and ammonium chloride (12.04 g, 225 mmol) in 150 mL of *N*,*N*-dimethylformamide was heated to 130°C and stirred for 72 hours in nitrogen atmosphere. The reaction mixture was then allowed to cool to room temperature and precipitated in 1200 mL of deionized (DI) water and subsequently acidified with dilute HCl. The precipitate was separated from the product via filtration, washed with DI water 3-4 times, and purified through base-acid (NH_4OH-HCl) extraction. The product was dried in a vacuum oven at 70°C. Yield: 17.20 g (76%); T_{melt}: 210.6-213.9°C. ^{1}H NMR (DMSO-d_6, δ): 8.65 (d, 1H, *J* 8.3 Hz), 8.31 (d, 1H, *J* 7.9 Hz), 7.97 (d, 1H, *J* 8.3 Hz), 7.76-7.59 (m, 2H), 7.20 (d, 1H, *J* 8.3 Hz), 4.08 (s, 3H).;

2-(4-methoxynaphthalen-1-yl)-5-(naphthalen-1-yl)-1,3,4-oxadiazole (3b) 3a (2.09 g, 9.1 mmol) was dissolved in pyridine (20 mL). Naphthoyl chloride (1.91 g, 10.01 mmol) was then added the reaction vessel. The reaction mixture was heated to reflux for 4 h. The solution was initially brown but became darker brown upon heating. Water (300 mL) was added to the cooled mixture to precipitate the pale yellow product. The product was recrystallized from a 1:1 EtOH:DMF solution. The crystallized product was vacuum filtered and washed with water (450 mL). The product was dried in air in the dark. Yield: 7.97 g (90.5%); T_{melt}: 180.2-181.5°C. ^{1}H NMR ($CDCl_3$, δ): 9.38 (d, 2H, *J* 8.6 Hz), 8.38 (d, 1H, *J* 8.6 Hz), 8.31-8.27 (dd, 2H), 8.04 (d, 1H, *J* 8.3 Hz), 7.94 (d, 1H, *J* 8.3 Hz), 7.78-7.68 (m, 2H), 7.65-7.55 (m, 3H), 6.92 (d, 1H), *J* 8.3 Hz), 4.08 (s, 3H).

4-[5-(naphthalen-1-yl)-1,3,4-oxadiazol-2-yl]-naphthalen-1-ol (3c) 3b (2.28 g, 6.47 mmol) was dissolved in hydroiodic acid 57 % wt (53.8 g, 421 mmol) distilled and stabilized with <1.5 % hypophosphorous acid. The reaction mixture was heated to 130 °C for 10 h. The reaction mixture was allowed to cool to room temperature and water (150 mL) was used to quench the reaction. The product was recrystallized out of a 1:1 acetic acid:DMF solution and was washed with copious amounts of water. The product was put in a desiccator in the dark to dry for 12 h. Yield: .561 g (26%); T_{melt}: 308.3-311.0°C. ^{1}H NMR (DMF-*d*7, δ): 11.50 (br. s, 1H), 9.44-9.35 (m, 2H), 8.49 (d, 1H), 8.45-8.36 (m, 2H), 8.26 (d, 1H, *J* 8.3 Hz), 8.14 (d, 1H, *J* 8.3 Hz), 7.85-7.60 (m, 5H), 7.20 (d, 1H, *J* 8.3 Hz).

4-[5-naphthalen-1-yl)-1,3,4-oxadiazol-2-yl] naphthalen-1-yl methacylate (MANON) 3c (.561 g, 1.66 mmol) and the catalyst, 4-dimethylaminopyridine (0.020 g, 0.164 mmol), were dissolved using elevated temperature in dioxane (dried over Na_2SO_4, 25 mL), and dry DMF (10 mL). The reaction flask was covered, and the vessel was purged with nitrogen for 10 min. The nitrogen purge was stopped and triethylamine (0.226 g, 2.23 mmol) was injected into the reaction vessel. The solution was a vibrant yellow. Methacryloyl chloride (0.217 g, 2.08 mmol) was injected drop wise into the reaction mixture. Upon the addition of methacryloyl chloride the solution turned brown. The reaction was stirred at room temperature for

approximately 60 hours. The reaction mixture was quenched with water (100 mL) and separated via filtration. The residue was washed with water. The product was recrystallized out of acetic acid and DMF. Yield: 91%; T_{melt}: 157.9-159.0°C(159.8°Cby DSC). FTIR (KBr): 3055, 1738 (ester), 1580 (oxadiazole), 1529, 1465, 1395, 1229, 1126, 1111, 806, 771 cm^{-1}. ^{1}H NMR ($CDCl_3$, δ): 9.46 (d, 1H, J 8.6 Hz), 9.37 (d, 1H, J 8.6 Hz), 8.37-8.28 (m, 2H), 8.09-8.00 (m, 2H), 7.95 (d, 1H), 7.80-7.69 (m, 2H), 7.68-7.57 (m, 3H), 7.48 (d, 1H), 6.57 (s, 1H), 5.92 (s, 1H), 2.19 (s, 3H). ^{13}C NMR ($CDCl_3$, δ): 165.3, 164.2, 163.8, 149.9, 135.5, 133.9, 132.7, 131.6, 130.2, 128.7, 128.6, 128.4, 128.2, 127.4, 127.3, 126.8, 126.7, 126.3, 124.9, 121.8, 120.4, 118.4, 117.5, 18.5. Elemental analysis (mass %) for $C_{26}H_{18}N_2O_3$: C, (calc: 76.83); H, (calc: 4.46); N, (calc: 6.89).

Preparation of polymers and colloids.

All polymerizations were carried out in an analogous manner. For the PKNC terpolymer, **MAK**, (0.652 g, 2.33 mmol), **MAC6**, (0.0143 g, .033 mmol), **MANON**, (0.406 g, 1 mmol), and AIBN (16.4 mg, 0.1 mmol) were dissolved in chlorobenzene (7 mL). Polymerization was carried out in rubber septa sealed test tubes immersed in an oil bath. Reaction mixture was sparged with nitrogen for approximately two minutes prior to heating to remove oxygen from the reaction vessel. The solution was under constant stirred for 24 h at 70°C and then added dropwise into 200 mL of cold methanol. The polymer was further purified by three reprecipitations from chloroform into methanol and it was then allowed to dry overnight at 60°C in a vacuum oven before characterization. PKNC: Yield: 0.61 g; T_g: 156°C. FTIR (KBr): 3007, 1752 (ester), 1611 (oxadiazole), 1532, 1495, 1203, 1166, 1088, 805, 773 cm^{-1}. ^{1}H NMR ($CDCl_3$, δ): 9.35-9.28 (br.m, 1H), 8.09-6.84 (br. m, 11H), 4.35-3.87 (br. m, 4H). Molecular weight = 24,432 g/mol.

Polymer colloids were prepared using a miniemulsion technique. 75 mg of polymer was dissolved into 2 g $CHCl_3$. To the organic phase, an aqueous sodium dodecylsulfate (SDS) (Sigma-Alrich, used as received) solution (4 $g \cdot L^{-1}$) was placed on the organic phase. The biphasic mixture was exposed to 12 W ultrasonic agitation (VirSonic Tip Sonicator) for 240 s. Following emulsion of the polymer, residual $CHCl_3$ is allowed to evaporate and the resulting aqueous dispersion is dialyzed against deionized water to remove residual SDS.

4.4 Device Fabrication.

The ITO was templated to a 12 mm^2 rectangular pattern and cleaned by successive immersions in acetone (Sigma Aldrich, used as received) and 2-propanol (Fisher Scientific, used as received). Both solvent baths were exposed to ultrasonic agitation. Devices were then dried under a N_2 stream. In order to remove residual organic material, the substrates were then exposed to an air plasma for 5 minutes, rinsed with deionized water and placed on a 125°C hotplate for 3 minutes to remove any moisture.

For spin cast devices, the prepared polymer solution was spin cast onto the templated ITO to a thickness of *ca.* 100 nm. The Al was deposited onto the polymer film to a thickness of *ca.* 200 nm by resistive evaporation (Denton model DV-502/DV-502A, deposition monitored by a Sigma Instruments QCM crystal thickness monitor). Printed devices were built on a PET substrate coated with In_2O_3/Au/Ag (Delta Technolgoies), $R_S \leq 10\Omega$. To avoid the introduction of dielectric layers, the In_2O_3/Au/Ag was templated similarly to the ITO coated on glass, and cleaned consistent with the rigid substrate samples. The colloidal ink was dropped onto the In_2O_3/Au/Ag and drawn with a wire–wound coating rod to simulate roll–to–roll printing (rod size 2.5, Paul N. Gardner Co.). In order to analyze the material as a printable ink, the cathode material (Al) was thermally evaporated to eliminate the variable of successive layer printing.

Device Characterization. Devices were connected to a computer controlled HP 4145a Semiconductor Parameter Analyzer using a J Microtechnology LS 110 probe station. The Al electrode was exposed to the applied biases while the ITO electrode remained tied to ground. All data were taken at a temperature of 23 °C in no light conditions unless otherwise noted.

5 Acknowledgements

The authors thank the Gregg-Graniteville Foundation for financial support.

References Cited

[1] M. Pudas, N. Halonen, P. Granat, and J. Vahakangas. Gravure printing of conductive particulate polymer inks on flexible substrates. *Progress in Organic Coatings*, 54:310–316, 2005.

[2] J. A. Rogers, Z. N. Bao, A. Makhija, and P. Braun. Printing process suitable for reel-to-reel production of high-performance organic transistors and circuits. *Advanced Materials*, 11:741–745, 1999.

[3] T. Makela, S. Jussila, H. Kosonen, T. G. Backlund, H. G. O. Sandberg, and H. Stubb. Utilizing roll-to-roll techniques for manufacturing source-drain electrodes for all-polymer transistors. *Synthetic Metals*, 153:285–288, 2005.

[4] B. Cho, S. Song, Y. Ji, T. W. Kim, and T. Lee. Organic resistive memory devices: Performance enhancement, integration, and advanced architectures. *Advanced Functional Materials*, 21:2806–2829, 2011.

[5] Tatiana Berzina, Anteo Smerieri, Marco Bernabo, Andrea Pucci, Giacomo Ruggeri, Victor Erokhin, and M. P. Fontana. Optimization of an organic memristor as an adaptive memory element. *Journal of Applied Physics*, 105:124515, 2009.

[6] E. T. Kang, S. L. Lim, Q. D. Ling, E. Y. H. Teo, C. X. Zhu, D. S. H. Chan, and K. G. Neoh. Conformation-induced electrical bistability in non-conjugated polymers with pendant carbazole moieties. *Chemistry of Materials*, 19:5148–5157, 2007.

[7] Y. K. Fang, C. L. Liu, and W. C. Chen. New random copolymers with pendant carbazole donor and 1,3,4-oxadiazole acceptor for high performance memory device applications. *Journal of Materials Chemistry*, 21:4778–4786, 2011.

[8] S. L. Lim, Q. D. Ling, E. Y. H. Teo, C. X. Zhu, D. S. H. Chan, E. T. Kang, and K. G. Neoh. Conformation-induced electrical bistability in non-conjugated polymers with pendant carbazole moieties. *Chemistry of Materials*, 19:5148–5157, 2007.

[9] K. Landfester. Synthesis of colloidal particles in miniemulsions. *Annual Review of Materials Research*, 36:231–279, 2006.

[10] M. E. Woods, J. S. Dodge, I. M. Krieger, and P. E. Pierce. Monodisperse latices .i. emulsion polymerization with mixtures of anionic and nonionic surfactants. *Journal of Paint Technology*, 40:541, 1968.

[11] Y. S. Papir, M. E. Woods, and I. M. Krieger. Monodisperse latices .3. cross linked polystyrene latices. *Journal of Paint Technology*, 42:571, 1970.

[12] Jiangshan Chen and Dongge Ma. Performance improvement by charge trapping of doping fluorescent dyes in organic memory devices. *Journal of Applied Physics*, 100, 2006.

[13] L. Micaroni, F. C. Nart, and I. A. Hummelgen. Considerations about the electrochemical estimation of the ionization potential of conducting polymers. *Journal of Solid State Electrochemistry*, 7:55–59, 2002.

[14] D. D Evanoff, Jr., J. B. Carroll, R. D. Roeder, Z. J. Hunt, J. R. Lawrence, and S. H. Foulger. Poly(methyl methacrylate) copolymers containing pendant carbazole and oxadiazole moieties for applications in single-layer organic light emitting devices. *Journal of Polymer Science Part A-Polymer Chemistry*, 46:7882–7897, 2008.

[15] Q. D. Ling, Y. Song, S. L. Lim, E. Y. H. Teo, Y. P. Tan, C. X. Zhu, D. S. H. Chan, D. L. Kwong, E. T. Kang, and K. G. Neoh. A dynamic random access memory based on a conjugated copolymer containing electron-donor and -acceptor moieties. *Angewandte Chemie-International Edition*, 45:2947–2951, 2006.

[16] R. Schmechel and H. von Seggern. Electronic traps in organic transport layers. *Physica Status Solidi a-Applied Research*, 201:1215–1235, 2004.

[17] Ireneusz Glowacki and Zbigniew Szamel. The nature of trapping sites and recombination centres in pvk and pvk-pbd electroluminescent matrices seen by spectrally resolved thermoluminescence. *Journal of Physics D-Applied Physics*, 43, 2010.

[18] G. Safoula, K. Napo, J. C. Bernede, S. Touihri, and K. Alimi. Electrical conductivity of halogen doped poly(n-vinylcarbazole) thin films. *European Polymer Journal*, 37:843–849, 2001.

[19] D. Bahnemann, A. Henglein, J. Lilie, and L. Spanhel. Flash-photolysis observation of the absorption-spectra of trapped positive holes and electrons in colloidal tio2. *Journal of Physical Chemistry*, 88:709–711, 1984.

[20] G. Rothenberger, J. Moser, M. Gratzel, N. Serpone, and D. K. Sharma. Charge carrier trapping and recombination dynamics in small semiconductor particles. *Journal of the American Chemical Society*, 107:8054–8059, 1985.

[21] F. C. Chen and H. F. Chang. Photoerasable organic nonvolatile memory devices based on hafnium silicate insulators. *Ieee Electron Device Letters*, 32:1740–1742, 2011.

[22] P. C. Johnson and H. W. Offen. Excimer fluorescence of poly(n-vinylcarbazole). *J. Chem. Phys.*, 55:2945–2949, 1971.

[23] D. J. Williams, W. W. Limburg, J. M. Pearson, A. O. Goedde, and J. F. Yanus. Electrical properties of a series of carbazole polymers. *Journal of Chemical Physics*, 62:1501–1506, 1975.

[24] M. Skompska and L. M. Peter. Electrodeposition and electrochemical properties of poly(n-vinylcarbazole) films on platinum-electrodes. *Journal of Electroanalytical Chemistry*, 383:43–52, 1995.

[25] J. A. Cheng, C. P. Chang, C. H. Chen, and M. S. Lin. The fluorescent quantum efficiency of copolymers containing coumarin-6 at the side-chain. *Journal of Polymer Research*, 12:53–59, 2005.

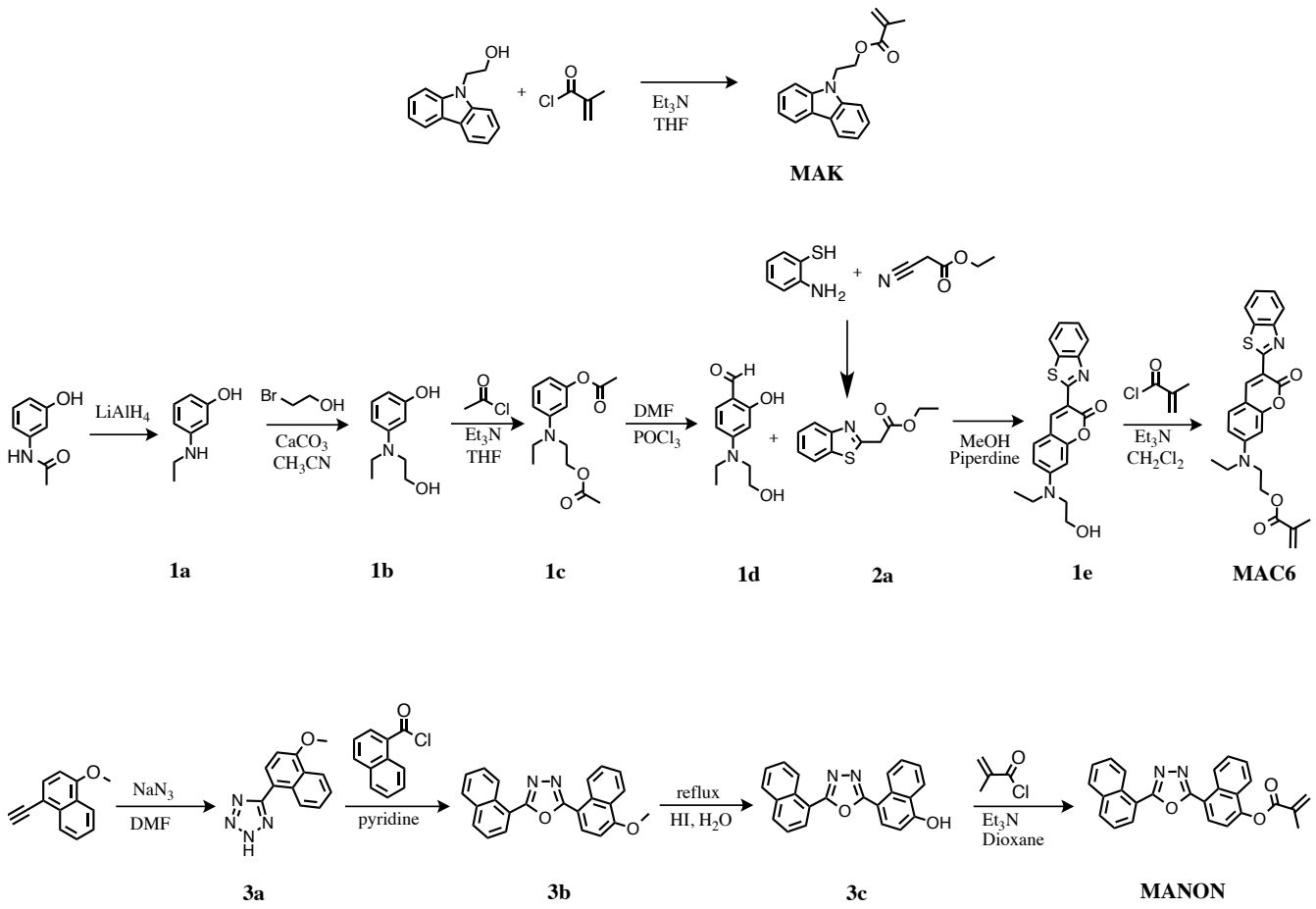

Figure 7: Synthetic scheme for MAK, MANON, and MAC6 monomers.